Optimizing Perpendicular Flux in PCB Embedded Inductors via Shift-Angle Topologies under DC Excitation

Mohamed ALKURDI [1,2], Christian MARTIN[3], Mounira BOUARROUDJ[1,4] and Mickael PETIT[1,5]
[1] *SATIE,* [2]*CNRS, Université Paris-Saclay,* [3] *Ampère, Université Claude Bernard Lyon 1,* [4]*Universite Paris Est Créteil,* [5] *CNAM*

ABSTRACT - The integration of magnetic components into printed circuit boards (PCBs) presents a promising solution for enhancing electromagnetic performance while minimizing space and manufacturing complexity in power electronics. A key challenge in this domain is the angular misalignment of inductor turns relative to the magnetic core centerline—often inevitable due to PCB manufacturing constraints. This misalignment distorts the magnetic field, increasing the perpendicular (Z-direction) magnetic flux density through copper traces and leading to elevated eddy current losses, leading to elevated eddy current losses in AC applications.

This study investigates various angle alignment topologies in PCB-embedded solenoid inductors to mitigate electromagnetic losses and optimize inductive performance. To isolate the influence of angular alignment from frequency-dependent phenomena like skin effect, proximity effect, and core losses, simulations were conducted under DC conditions using Ansys Maxwell. Several angular configurations were analyzed to evaluate their effects on flux distribution and eddy current formation.

Results indicate that altering the angle alignment significantly impacts flux behavior, with Configuration 2 (A = -Q), featuring two opposite angles symmetrically placed at the midpoint of the turns, demonstrating the lowest flux loss and eddy current dissipation. Experimental validation confirmed the simulation findings, showing electromagnetic losses remained within a 6% margin.

This study confirms that optimizing turn alignment can substantially improve the efficiency of PCB-integrated inductors. Future work will explore further enhancements through advanced winding techniques (e.g., litz wire), alternative geometries (e.g., toroidal shapes), and the integration of active components for high-frequency, high-efficiency converter applications.

Keywords—Embedded magnetics, PCB Inductor, Toroidal Core, Flux Leakage, Magnetics Simulation, Alignment optimization.

1. INTRODUCTION

The integration of magnetic components into printed circuit boards (PCBs) along with other electronic components has become a focal point in power electronics research, particularly for static converter applications as shown in Fig. 1.

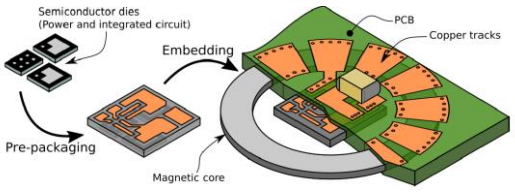

Fig. 1 Integration of power dies and integrated circuits together in a common "pre-package", which is then embedded, together with large magnetic components, in a PCB to form a complete converter

Embedding magnetic components within PCBs offers numerous advantages, including reduced size, improved electromagnetic compatibility (EMC), and enhanced thermal management[1].

Among the various magnetic core designs, toroidal cores are widely preferred due to their ability to confine magnetic flux within the core, thereby minimizing electromagnetic interference (EMI) as the study result in Fig. 2[2].

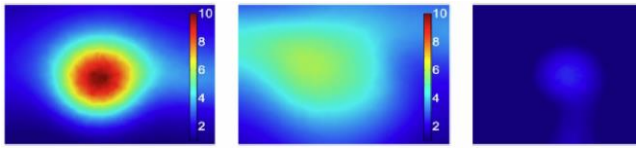

Fig. 2 Magnetic field (A/m) 2mm above of PCB embedded air core inductors [2].

However, embedding toroidal cores introduces significant challenges, particularly in the precise alignment of inductor turns with the core centerline similar to Fig. 3[3].

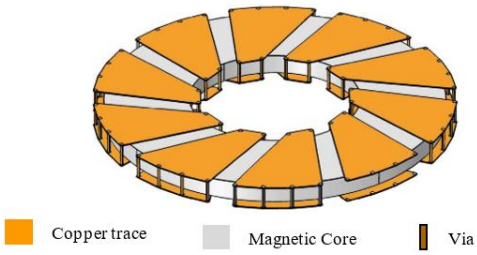

Fig. 3 Embedded PCB toroidal inductor design[3].

Achieving perfect alignment is difficult due to manufacturing limitations, leading to a misalignment angle that distorts the magnetic field distribution. This distortion causes an increase

of perpendicular component of the flux in the copper turns, which can induce higher eddy currents and reduce efficiency in AC applications. Eddy current losses, a major concern in high-frequency power electronics, can significantly impact the performance and thermal problems of embedded magnetic devices as shown in Fig. 4[4].

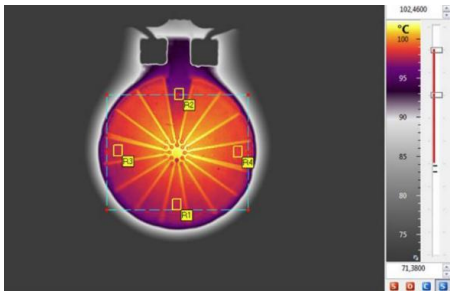

Fig. 4 Thermogram for 2.5A 5MHz embedded PCB inductor[4].

2. Problem Formulation

As a previous study has proved the relationship between the increase of the angle alignment value and the flux perpendicular to the copper turns to be incremental as illustrated in Fig. 5. This study comes to investigate different approaches to minimize the angle alignment effect [5].

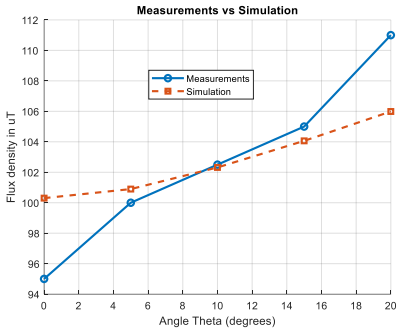

Fig. 5 The average of maximum flux density perpendicular to the middle traces (top PCB/bottom PCB) in lab measurements compared to simulation results.

These approaches are based on the angle location and layers. The top layer Angle is referenced (Q) while the bottom layer angle is referenced (A), so there are four approaches as listed in Fig. 6.

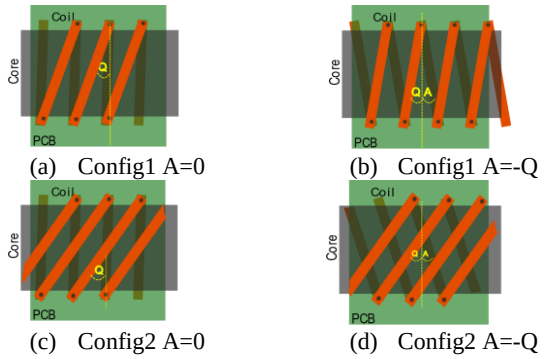

(a) Config1 A=0 (b) Config1 A=-Q

(c) Config2 A=0 (d) Config2 A=-Q

Fig. 6 Illustration of the four different design approaches for alignment angle configurations in embedded PCB inductors.

3. Model Simulation

Using Finite Element Method (FEM) simulations via Ansys Maxwell [6][7], the four proposed design approaches will be analyzed under DC sources. To ensure a fair comparison, all models will share identical boundary conditions and simulation parameters stated in Table I [8].

3.1. DC Simulation

The primary objective is to evaluate the relationship between the alignment angle and the flux density (Bz) perpendicular to the copper traces. Since some configurations have A = 0°, while others have A = -Q, the comparison will be conducted using the total alignment angle defined as:

$$\text{Total Angle} = Q + |A| \quad (1)$$

By using this metric, the study maintains a consistent turn-to-turn clearance across all configurations, ensuring that differences in flux behavior are attributed solely to the alignment angle variations rather than trace spacing inconsistencies [9].

Table I Simulation boundaries and parameters

Parameter	**Value**	**unit**
Current	1.4	A
Trace width	2	mm
Trace length	28	mm
Copper thickness	0.035	mm
Core thickness	2	mm
Core length	54	mm
Core permeability	26	
Core PN#	00K9541B026	
Clearance	8	mm
Number of turns	5	turn

In order to reduce the simulation time, the mesh is fined only in the middle trace for both layers and the measurements are done in it [10], so that the maximum element length of the mesh is 60µm as shown in Fig. 7, while the current path and magnetic field directions are shown in Fig. 8.

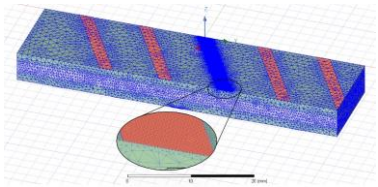

Fig. 7 Simulation model mesh

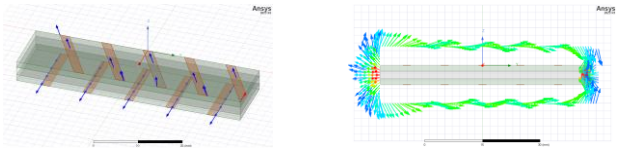

(a) (b)

Fig. 8 (a) The model current path, (b) Front view of the magnetic field direction

3.2. *DC Simulation Results*

In the simulation software it's possible to observe the Flux (Ø) in the z direction inside the copper [11], [12]. This can show the impact on eddy current formulation in AC application according to the following relationships:

$$\varepsilon = \frac{d\emptyset}{dt} \tag{2}$$

$$\emptyset = \oint \beta \, ds \tag{3}$$

$$P_e = K_e B^2 f^2 d^2 \tag{4}$$

Ɛ = Induced electromotive force (V), Φ = Magnetic flux (Wb), B = Magnetic flux density (T), ds = Differential surface element, P_e = Eddy current power loss (W/m³), K_e = Eddy current coefficient (material & geometry dependent), f = Frequency (Hz), d = Conductor thickness (m).

The results in Fig. 9 are flux in the middle traces versus the angle increase in each configuration, they indicate that Config.1 A=-Q and Config.2 A=-Q achieve similar levels of flux reduction, both outperforming Config.1 A=0 and Config.2 A=0. Among all configurations, Config.2 A=-Q proves to be the most effective in minimizing perpendicular flux density (Øz).

Specifically, for Config.2 A=-Q, the increase in (Øz) from 0° to 30° is only 3.7%, whereas for Config.1 A=0, the increase reaches 14.8%, highlighting the significant advantage of the A=-Q configuration in reducing flux-induced losses.

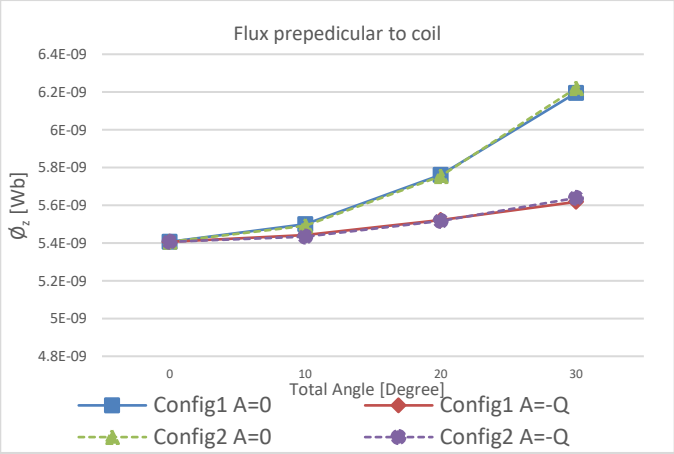

Fig. 9 Ansys Maxwell simulation results showing Config.2 A=-Q with the lowest perpendicular flux density

Fig. 10 illustrates the impact of counter angles (A = -Q) on the uniformity of the magnetic field distribution. The four subfigures (a), (b), (c), and (d) display the magnetic field behavior within the system, with color mapping representing the field intensity in microtesla (μT). The arrows indicate the field direction, while the color gradient from blue to red shows the field strength, with red indicating the highest intensity.

In subfigures (a) and (b), the angle position is located at the end of the trace, which leads to the formation of a vortex-like shape in the magnetic field at the right edge of the model. This vortex effect is visible through the swirling pattern of the field lines, which suggests localized field distortions. In contrast, in subfigures (c) and (d), the field appears more uniform, indicating a more stable and structured magnetic path.

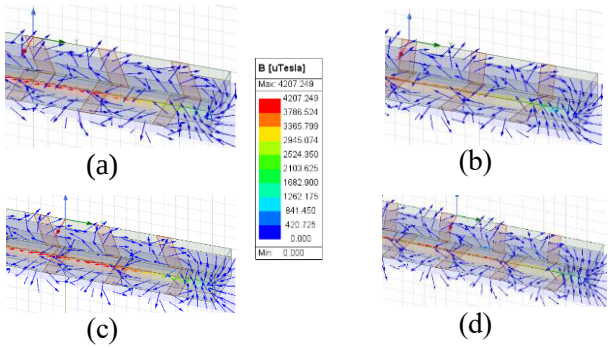

Fig. 10 Illustration of the magnetic field path and density in the simulation model (a) Config1 A=0, (b) Config 1 A=-Q, (c) Config 2 A=0, (d) Config 2 A=-Q

The use of counter angles contributes to the overall uniformity of the field, reducing irregularities and enhancing consistency, which is crucial for applications requiring controlled magnetic environments.

4. Experimental Validation

4.1. *PCB Design*

The PCBs are designed to implement the proposed approaches similar to Fig. 11, each incorporating a 5-turn embedded solenoid inductor. The design consists of:

- 5 traces on the top PCB layer
- 5 traces on the bottom PCB layer, both connected in series to ensure electrical continuity.

The middle section serves as the test area, and the connector is placed 47mm away to minimize any potential interference from radiated emissions. The PCBs were designed using Altium Designer, with a focus on Design for Testing (DFT), and they include designated positions for future BNC connectors [13].

In total, 20 PCB designs were developed, covering all the required test approaches.

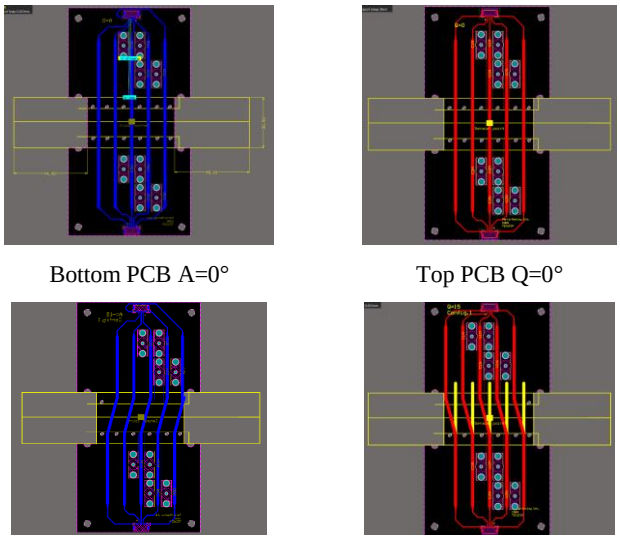

Bottom PCB A=0° Top PCB Q=0°

Bottom PCB Config1 A=-15° Top PCB Config1 Q=15°

Fig. 11 Examples of PCB Designs done in Altium SW

4.2. Experiment setup for DC test

A customized test setup in Fig. 12 has been developed to investigate the effect of angle alignment on magnetic flux density. The setup includes a plastic support structure designed to hold the printed circuit boards (PCBs) in place by aligning them with a magnetic core [14].

The system consists of three key components positioned within the holder:

1- Top Layer PCB – Serves as the upper conductive layer.
2- Magnetic Core – Centrally positioned to influence the magnetic flux.
3- Bottom Layer PCB – Completes the structure, ensuring a stable configuration.

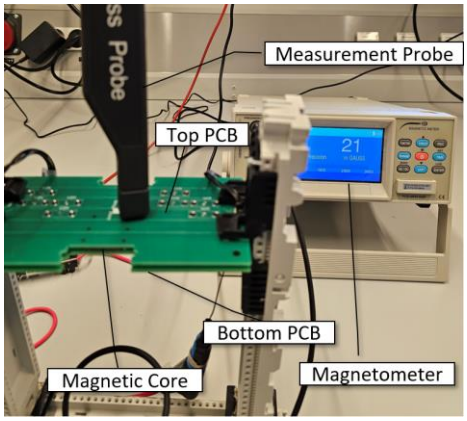

Fig. 12 Experimental set to validate the approaches measures

A PCE-MFM 4000-ICA magnetometer with a resolution of 0.01 µT is employed for high-precision measurements. Due to the small variations in flux density caused by angle alignments, a high-precision probe is utilized instead of the general probe to enhance sensitivity and detect subtle changes [15].

The high-precision probe is positioned vertically along the trace edge to measure the maximum perpendicular flux density (Bzmax). This ensures that the measurement captures the peak flux component in the perpendicular direction to the copper traces [16].

To systematically evaluate different angle configurations, each PCB is designed with a specific angular arrangement. When a particular angle configuration is tested, the corresponding PCBs are placed in the holder, and measurements are recorded accordingly. This method illustrated in Fig. 13 allows for a controlled investigation of the influence of PCB angle alignments on the observed magnetic flux density.

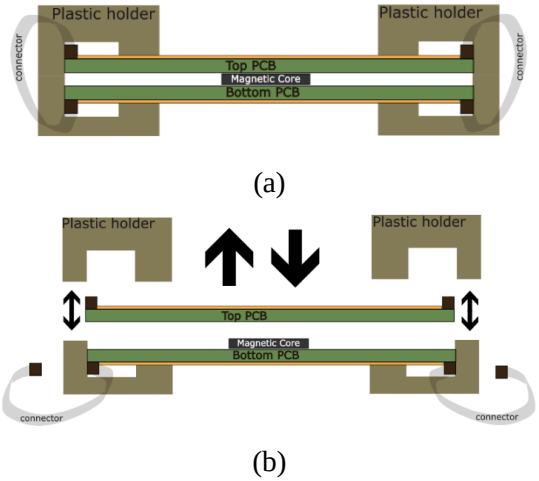

Fig. 13 (a) illustration of the experimental set structure, (b) The configuration changing mechanism

Measuring the total flux (Øz) is highly complex, as it requires sweeping the flux density (Bz) along the trace and performing an integral calculation over the trace surface. To simplify the process and obtain a more practical and reliable measurement, the approach focuses on measuring the maximum flux density (Bz max) instead.

For accuracy and consistency, flux density measurements are taken at four key points—positioned at the edges of the trace as shown in Fig. 14, where the magnetometer detects the highest Bz values. The average of these four measurements is then calculated to ensure a precise and representative result. The probe measures the perpendicular flux density (Bz) on the copper traces.

Due to the plastic casing of the probe, the internal sensor is positioned 4 mm above the edge of the copper trace. Therefore, for an accurate comparison with simulation readings, measurements should be taken at the same 4 mm height above the copper trace in the simulation, as illustrated in Fig. 14[17].

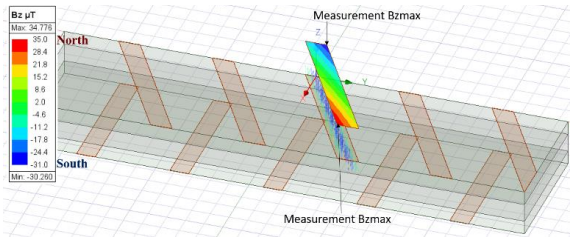

Fig. 14 Simulation model illustrating the measurement of perpendicular flux density (Bz) on the copper traces.

Adding a 1-ohm series resistor in the circuit as in Fig. 15 helps stabilize the current during the DC testing of the inductor [18]. Since the inductor has a very low DC resistance, it can cause high current draw, potentially leading to power supply instability or current surges. The series resistor mitigates this issue by:

- Limiting Inrush Current – Prevents excessive current flow when the circuit is powered on.
- Improving Stability – Reduces fluctuations in the power supply, ensuring more consistent current.
- Enhancing Measurement Accuracy – Helps maintain controlled test conditions by preventing rapid variations in current.

In essence, this resistor acts as a current stabilizer to protect both the power supply and the inductor while maintaining controlled test conditions [19].

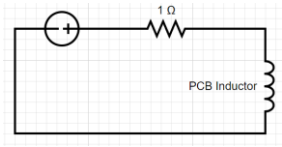

Fig. 15 Experimental setup circuit diagram

4.3. Experimental results

Fig. 16 presents a comparison between experimental and simulated results, analyzing the impact of different angle configurations on the maximum flux density. The results validate the simulation model, demonstrating that Configuration 2 (A = -Q) achieves the best performance.

Fig. 16 Comparison of experimental and simulation results for different angle configurations

The experimental data (solid lines) exhibit more variability than the simulation data (dashed lines). The average difference between experimental and simulated results is 2–4 µT, within the expected measurement error range of ±2 µT.

These results confirm that the simulation effectively represents real-world behavior, with Configuration 2 (A = -Q) emerging as the optimal approach for enhancing the uniformity and intensity of the magnetic flux.

5. CONCLUSION

This study investigated the impact of angle alignment topologies on flux distribution in PCB-embedded solenoid inductors. To ensure an isolated evaluation of the angle alignment design approaches, the study employed DC power supply instead of AC. This choice effectively eliminated the skin effect, proximity effect, core loss, and other interfering factors, allowing for a precise analysis of how different alignment configurations influence flux behavior that can cause eddy current formation.

Simulation and experimental results confirmed that Configuration 2 (A = -Q) consistently exhibited the lowest flux perpendicular to the coil traces, making it the most efficient design for minimizing electromagnetic losses. Experimental validation further demonstrated that electromagnetic losses remained within a 6% margin, ensuring that the proposed configurations are viable for real-world implementations.

Future research will focus on enhancing inductor design efficiency through multiple approaches:

- Exploring Alternative Designs: Investigating different design methodologies, including the use of litz wire, to reduce eddy current losses and improve high-frequency performance.
- Expanding to Other Inductor Shapes: Evaluating the implementation of toroidal inductors, assessing their feasibility and performance under various design constraints.
- Studying Angle Effects in AC Applications: Analyzing how angle alignments influence performance under AC excitation, considering skin effect, proximity effect, and electromagnetic losses.
- Integrating Active Components in Toroidal Inductors: Investigating the potential co-integration of active components to enhance functionality and optimize power efficiency.
- Assessing Thermal Behavior: Examining the heat dissipation characteristics of different configurations to ensure thermal stability and long-term reliability.

By addressing these aspects, the study aims to develop more efficient, scalable, and high-performance embedded inductor solutions for advanced static converters applications.

6. ACKNOWLEDGEMENT

This study is part of PhD program funded by ANR in the frame of TECoCIP Project in coordination with CNRS, SATIE lab in ENS Paris-Saclay and Ampére lab in Lyon.

7. REFERENCES

[1] by Neel Mayur Shah and B. Parkhideh Badrul Chowdhury Jonathan Bird, "INVESTIGATION ON TOROIDAL PCB EMBEDDED INDUCTOR FOR POWER ELECTRONICS APPLICATIONS," The University of North Carolina at Charlotte, 2015.

[2] M. Madsen, A. Knott, M. A. E. Andersen, and A. P. Mynster, "Printed circuit board embedded inductors for very high frequency Switch-Mode Power Supplies," in *2013 IEEE ECCE Asia Downunder*, IEEE, Jun. 2013, pp. 1071–1078. doi: 10.1109/ECCE-Asia.2013.6579241.

[3] R. Caillaud *et al.*, "Design, manufacturing and characterization of printed circuit board embedded inductors for power applications," in *2018 IEEE International Conference on Industrial Technology (ICIT)*, IEEE, Feb. 2018, pp. 694–699. doi: 10.1109/ICIT.2018.8352262.

[4] G. Weidinger *et al.*, "New Embedded Inductors For Power Converter Applications," in *Minapad 2018*, Grenoble; France, May 2018. [Online]. Available: www.ats.net

[5] M. Alkurdi, C. Martin, M. Bouarroudj, and M. Petit, "Investigating the Impact of Alignment Angle Between Copper Turns and Magnetic Core on Magnetic Field Coupling in PCB Integrated Inductors," Paris: EPE25, Apr. 2025.

[6] J. P. A. Bastos and N. Sadowski, *Magnetic Materials and 3D Finite Element Modeling*. CRC Press, 2017. doi: 10.1201/b15558.

[7] Inc. ANSYS, "HFSS Fields Calculator Cookbook," 2017. [Online]. Available: http://www.ansys.com

[8] Zeeshan Umar, "Design of an Embedded PCB Inductor with a Ferrite Magnetic Core for Power Applications Design," Nuremberg, Apr. 2024. Accessed: Jan. 27, 2025. [Online]. Available: https://d-nb.info/134898421X/34

[9] R. R. Tummala, M. Swaminathan, S. Suresh, and H. Garmestani, "Modeling, Design and Fabrication of Substrate-Embedded Inductors with High Inductance Density and Low DC Resistance for Integrated Voltage Regulators," TEXT, Georgia Institute of Technology, Georgia, 2020.

[10] Rasha Saeed, "Design and Characterisation of a High Energy-Density Inductor," University of Nottingham, Nottingham, 2017.

[11] L. Yan *et al.*, "Research on Simultaneous Measurement of Magnetic Field and Temperature Based on Petaloid Photonic Crystal Fiber Sensor," *Sensors*, vol. 23, no. 18, p. 7940, Sep. 2023, doi: 10.3390/s23187940.

[12] M. P. Madsen, J. D. Mønster, A. Knott, and M. A. E. Andersen, "Design Optimization of Printed Circuit Board Embedded Inductors through Genetic Algorithms with Verification by COMSOL," in *The 2013 COMSOL Conference in Boston*, Boston: 2013 COMSOL Conference in Boston, 2013.

[13] Mohamed Alkurdi, "Enhancement of Electromagnetic Interference Control Techniques Using Printed Circuit Boards Design," Thesis, Aswan university, Aswan, 2023. doi: 10.13140/RG.2.2.36302.16960.

[14] Tumanski S, "Modern magnetic field sensors – a review," *Electrotechnical Review*, vol. 89, no. 10, pp. 1–12, 2013.

[15] V. Gurusamy, G.-A. Capolino, B. Akin, H. Henao, R. Romary, and R. Pusca, "Recent Trends in Magnetic Sensors and Flux-Based Condition Monitoring of Electromagnetic Devices," *IEEE Trans Ind Appl*, vol. 58, no. 4, pp. 4668–4684, Jul. 2022, doi: 10.1109/TIA.2022.3174804.

[16] Munima Haque, Quamruzzaman Mohammad, and Shahina Haque, "Measurement of Magnetic Field Emitted from Electrical Appliances in CSE Labs and Classrooms of Southeast University, Bangladesh," *Int J Sci Eng Res*, vol. 7, no. 10, pp. 295–304, Oct. 2016.

[17] M. Ludwig, M. Duffy, T. O'Donnell, and C. O'Mathuna, "Design study for ultra-flat, PCB integrated inductors for low power conversion applications," in *Digests of the Intermag Conference*, Institute of Electrical and Electronics Engineers Inc., 2003. doi: 10.1109/tmag.2003.816055.

[18] K. Zheng *et al.*, "PCB-embedded solenoid inductors with different magnetic cores," *Journal of Power Electronics*, vol. 24, no. 12, pp. 1990–1999, Dec. 2024, doi: 10.1007/s43236-024-00861-x.

[19] V. Solberg, "Embedding Passive and Active Components: PCB Design and Fabrication Process Variations," in *IPC APEX EXPO Conference Proceedings*, 2015.